

*Electronic Supplementary Information*

**Styrylcyanine-based ratiometric and tunable fluorescent pH sensors**

Abhineeshbabu Thottiparambil,<sup>a</sup>Anil Kumar PR,<sup>b</sup> Lakshmi Chakkumkumarath <sup>\*a</sup>

<sup>†</sup> Department of Chemistry, National Institute of Technology Calicut, Kerala, India-673601

<sup>‡</sup> Tissue Culture Laboratory, Biomedical Technology Wing, Sree Chitra Tirunal Institute for Medical Sciences and Technology, Thiruvananthapuram, Kerala, India – 695012.

E-mail: [lakshmic@nitc.ac.in](mailto:lakshmic@nitc.ac.in)

---

<b>Contents</b>	<b>Page</b>
Experimental details and spectral data	<b>3-5</b>
Fig. S1. ORTEP view of compounds <b>2</b> (a) and <b>3</b> (b) with atom numbering	<b>5</b>
Table S1. X-Ray crystallographic data and structure refinement details for <b>2</b> and <b>3</b> .	<b>6</b>
Table S2. Photophysical properties of <b>1</b> , <b>2</b> , and <b>3</b>	<b>7</b>
Fig. S2. Excitation and emission spectra of <b>1</b> , <b>2</b> & <b>3</b> in BR buffer	<b>8</b>
Fig. S3. Ratiometric response curves of <b>1</b> showing variation in $A_{355}/A_{409}$ (a) and $A_{416}/A_{355}$ (b) with pH.	<b>9</b>
Fig. S4. Fluorescence emission spectra of <b>1</b> ( $\lambda_{\text{ex}}$ : 409nm, $3.3 \times 10^{-5}\text{M}$ ) in BR buffer at various pH (pH 2.5- 6.75).	<b>9</b>
Fig. S5. (a) Change in emission intensity ( $\lambda_{\text{ex}}$ 409 nm, $\lambda_{\text{em}}$ 560 nm) of $3.3 \times 10^{-5}\text{M}$ solution of <b>1</b> with pH; b) Plot of normalized fluorescence vs. pH.	<b>10</b>
Fig. S6: (a) Cycle index of <b>1</b> between pH 7.5 and 10.5; (b) Time dependent emission intensities of <b>1</b> at different pH.	<b>10</b>
Fig. S7. Ratiometric response curve of <b>2</b> showing variation in a) $A_{366}/A_{430}$ and b) $A_{434}/A_{366}$ with pH.	<b>11</b>
Fig. S8. Plot of normalized fluorescence intensity vs pH for compound <b>2</b> .	<b>11</b>
Fig. S9. Time dependent fluorescent emission of $3.3 \times 10^{-5}\text{M}$ solution of <b>2</b> in BR buffer	<b>11</b>

at pH 3.63, 6.5 and 9.0 for 140 min ( $\lambda_{\text{ex}} = 410$  nm and  $\lambda_{\text{em}} = 518$  nm).

Fig. S10. Fluorescence emission spectra of $3.3 \times 10^{-5}$ M solution of <b>3</b> ( $\lambda_{\text{ex}}$ : 380 nm) in BR buffer	12
Fig. S11. a) Time-depedent emission and b) absorption spectra of <b>3</b> in BR buffer ( $3.3 \times 10^{-5}$ M, pH 2.50, $\lambda_{\text{exc}}$ 380 nm).	12
Fig. S12. Time-dependent changes in the intensity of fluorescent emission of <b>3</b> ( $3.3 \times 10^{-5}$ M) in BR buffer at pH 2.62 for 60 min ( $\lambda_{\text{ex}} = 480$ nm and $\lambda_{\text{em}} = 605$ nm).	12
Fig. S13. Fluorescence intensities of solutions of <b>1</b> & <b>2</b> in BR buffer in presence of various metal ions (10 equivalents)	13
Cytotoxicity and Dose Response Analysis of <b>2</b>	13-16
Confocal microscope imaging studies of compound <b>2</b> in HepG2 cells	17-18
Fig. S21. $^1\text{H}$ NMR of <b>1</b> (500 MHz, $\text{CDCl}_3$ ).	19
Fig. S22. $^{13}\text{C}$ NMR of <b>1</b> (125 MHz, $\text{CDCl}_3$ ).	19
Fig. S23. $^1\text{H}$ NMR of <b>2</b> (500 MHz, $\text{CDCl}_3$ ).	20
Fig. S24. $^{13}\text{C}$ NMR of <b>2</b> (125MHz, $\text{CDCl}_3$ ).	21
Fig. S25. HRMS of <b>1</b> .	21
Fig. S26. HRMS of <b>2</b> .	22

## General Information

$^1\text{H}$  and  $^{13}\text{C}$  NMR spectra were recorded on Bruker 500 MHz instrument and chemical shift are reported in parts per million (ppm) relative to tetramethylsilane (TMS) standard, with J values in Hz. Splitting patterns in  $^1\text{H}$  NMR are reported as follows: s (singlet), bs (broad singlet), t (triplet), dd (doublet of doublet); dt (doublet of triplet); app t (apparent triplet), app dt (apparent doublet of triplet) etc.  $^{13}\text{C}$  peaks are reported with solvent peak ( $\text{CDCl}_3 = 77.0$ ) as internal standard. High-resolution mass spectra (HRMS) were recorded on a Water Q-ToF *micro*<sup>TM</sup> spectrometer with lock spray source. Absorption spectra were recorded on a Shimadzu UV 2450 spectrometer. Fluorescence spectra were recorded on a Perkin Elmer LS-45 fluorescence spectrometer. Single crystal X-ray analysis was performed on Bruker Kappa Apex2 CCD Diffractometer. Cellular uptake was analyzed using a Laser Scanning Confocal Microscope (LSM 510 Meta, Carl Zeiss, Germany)

All the reagents and solvents were purchased from Sigma and Merck and used without further purification unless otherwise mentioned. THF was dried by distillation from sodium wire-benzophenone prior to use.  $\text{CH}_2\text{Cl}_2$  was distilled from  $\text{CaH}_2$ , and DIPEA was distilled over KOH. Thin layer chromatography was performed on silica gel plates (60 F254 0.25 mm from Merck) and components were analysed using UV light or by treating tlc plates with  $\text{KMnO}_4$  solution or Iodine. Chromatographic separation was carried out on 100-200 mesh silica gel. The Britton-Robinson buffer was prepared by mixing equal volume of 0.04 M acetic acid, 0.04 M phosphoric acid, and 0.04 M boric acid. The desired pH was obtained by addition of 0.5 M NaOH or 0.5 M HCl. The stock solutions of the pH probes **1-3** ( $10^{-3}\text{M}$ ) were prepared in DMSO. The test solution was prepared by diluting 100  $\mu\text{l}$  of the stock solution with 3 mL of Britton-Robins buffer. The slit width was kept at 10 nm during both excitation and emission measurements. All pH measurements were carried out using pH meter MK-VI (pH range: 0-14, resolution: 0.1pH). All data were processed with Origin 8.0

L-929 mouse fibroblast cells (CCL-1) was purchased from American Type Cell Culture, USA and Human liver hepatocellular cells (HepG2) was purchased from National Centre for Cell Science, Pune. Minimum Essential Medium (MEM), Antibiotics (Penicillin - 100 IU/ml and Streptomycin – 100  $\mu\text{g}/\text{ml}$ ), 3-(4, 5-Dimethyl thiazol -2-yl)-2,5- diphenyltetrazolium bromide (MTT) and dimethyl sulfoxide (DMSO) and Propidium Iodide (PI) were procured from Sigma, India. Foetal Bovine Serum (FBS) and Trypsin-EDTA (0.2%-0.02%) was purchased from Gibco, India. Cell cultureware was obtained from Nunc. All other chemicals were of analytical grade and obtained from Merck, India.

### General method for synthesis of compounds 1-3.

2,3,3-trimethyl indolenine (3.14 mmol) and DIPEA (3.46 mmol) were mixed in ethanol (5 mL) and refluxed for one hour. The appropriate aldehyde (3.46 mmol) was slowly added to the reaction mixture, at 85°C and stirred for 20 h. The reaction mixture was then cooled to room temperature and solvent was removed. The crude product was then purified on a silica gel column using hexanes/ethyl acetate as eluent.

**Compound 1:** Yield: 58%; IR (KBr)  $\text{cm}^{-1}$ : 3421, 2960, 2923, 1746, 1619, 1375, 1152;  $^1\text{H}$  NMR (500 MHz,  $\text{CDCl}_3$ ):  $\delta$  1.50 (s, 6H, 2 x  $\text{CH}_3$ ), 6.86 (app t, 1H,  $J = 7.5$ , 7.5 Hz, ArH), 7.00 (d, 1H,  $J = 6.5$  Hz), 7.14-7.18 (m, 1H, ArH), 7.28 (app dt, 1H,  $J = 7.5$ , 7.5, 1Hz, ArH), 7.37-7.41 (m, 2H, ArH), 7.42 (d, 1H,  $J = 16.5$  Hz, olefinic CH), 7.55 (dd, 1H,  $J = 8$ , 1.5 Hz), 7.73 (d, 1H,  $J = 7.5$  Hz), 8.36 (d, 1H,  $J = 16.5$  Hz, olefinic CH), phenolic OH was not observed;  $^{13}\text{C}$  NMR (125 MHz,  $\text{CDCl}_3$ )  $\delta$  24.1 (2C), 52.6, 117.0, 118.0, 119.5, 119.6, 121.4, 123.5, 125.6, 128.0, 128.5, 130.8, 137.4, 146.3, 152.4, 157.2, 185.7; HRMS (ESI) exact mass calcd. for  $\text{C}_{18}\text{H}_{18}\text{NO}$   $[\text{M}+\text{H}]^+$  264.1388, found  $[\text{M}+\text{H}]^+$  264.1386.

### Compound 2:

Yield: 52%; IR (KBr)  $\text{cm}^{-1}$ : 3442, 2924, 1747, 1589, 1384, 1212, 1160, 1026;  $^1\text{H}$  NMR (500 MHz,  $\text{CDCl}_3$ ):  $\delta$  1.51 (s, 6H, 2 x  $\text{CH}_3$ ), 3.78 (s, 3H,  $-\text{OCH}_3$ ), 6.78 (dd, 1H,  $J = 8.5$ , 3 Hz, ArH), 6.90 (d, 1H,  $J = 8.5$  Hz, ArH), 7.09 (d, 1H,  $J = 3$  Hz, ArH), 7.28 (d, 1H,  $J = 16.5$  Hz, olefinic CH), 7.29 (app dt, 1H,  $J = 7.5$ , 7.5, 1 Hz, ArH), 7.39 (d, 1H,  $J = 7.5$  Hz, ArH), 7.40 (app dt, 1H,  $J = 7.5$ , 7.5, 1Hz, ArH), 7.73 (d, 1H,  $J = 7.5$  Hz, ArH), 8.36 (d, 1H,  $J = 16.5$  Hz, olefinic CH), phenolic OH was not observed;  $^{13}\text{C}$  NMR (125 MHz,  $\text{CDCl}_3$ ):  $\delta$  23.99 (2C), 52.62, 55.87, 112.07, 117.21, 117.78, 118.00, 119.71, 121.42, 123.94, 125.66, 127.94, 136.63, 146.25, 151.22, 152.51, 152.79, 185.37; HRMS (ESI): exact mass calcd for  $\text{C}_{19}\text{H}_{20}\text{NO}_2$   $[\text{M}+\text{H}]^+$  294.1494, found  $[\text{M}+\text{H}]^+$  294.1503.

### Compound 3:

Yield: 64%; IR (KBr)  $\text{cm}^{-1}$ : 3681, 3020, 2400, 2104, 1525, 1425, 1216, 1044;  $^1\text{H}$  NMR (500 MHz,  $\text{CDCl}_3$ ):  $\delta$  1.56 (s, 6H, 2 x  $\text{CH}_3$ ), 7.02 (d, 1H,  $J = 9.2$  Hz), 7.30-7.47 (m, 4H, ArH + olefinic CH), 7.69 (d, 1H,  $J = 7.6$  Hz, ArH), 8.08 (dd, 1H,  $J = 9.2$ , 2.8 Hz, ArH), 8.37 (d, 1H,  $J = 16.4$  Hz, olefinic CH), 8.51 (d, 1H,  $J = 2.8$  Hz, ArH), phenolic OH was not observed;  $^{13}\text{C}$  NMR (125 MHz,  $\text{DMSO}-d_6$ ):  $\delta$  22.74 (2C), 52.38, 116.43, 120.166, 121.49, 121.57, 123.31, 123.63, 125.55, 125.91, 127.67, 130.62, 140.01, 146.69, 153.62, 162.10, 183.29; HRMS (ESI): exact mass calcd for  $\text{C}_{18}\text{H}_{17}\text{N}_2\text{O}_3$   $[\text{M}+\text{H}]^+$  309.1239, found  $[\text{M}+\text{H}]^+$  309.1241.

### Calculation of quantum yield

The quantum yields of **1** and **2** were calculated using the following equation.

$$\Phi_X = \Phi_R (I_X/I_R) (OD_R/OD_X) (n_X^2/n_R^2)$$

Where  $\Phi_R$  is the quantum yield of the standard, I is the integrated intensity, OD is the optical density, and n is the refractive index. X subscript denotes unknown, and R means standard. Quinine sulfate (0.1M H<sub>2</sub>SO<sub>4</sub>,  $\lambda_{ex}$ : 366nm,  $Q_R=0.53$ ) was used as the standard.

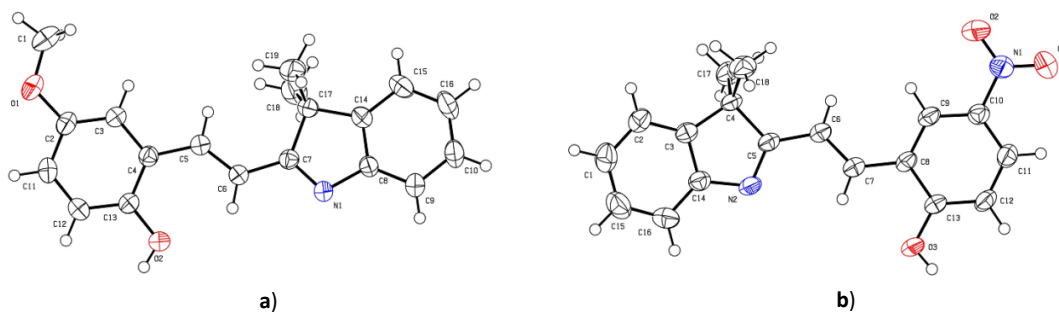


**Fig. S1.** ORTEP view of compounds **2** (a) and **3** (b) with atom numbering.

**Table S1.** X-Ray crystallographic data and structure refinement details for **2** and **3**.

	<b>Compound 2</b>	<b>Compound 3</b>
Empirical formula	C <sub>19</sub> H <sub>19</sub> N O <sub>2</sub>	C <sub>18</sub> H <sub>16</sub> N <sub>2</sub> O <sub>3</sub>
Formula weight	293.35	308.33
Temperature	296(2) K	296(2) K
Wavelength	0.71073 Å	0.71073 Å
Crystal system	Monoclinic	Monoclinic
space group	P21/n	P21/n
Unit cell dimensions	a = 15.852(5) Å $\alpha = 90^{\circ}$ . b = 6.0728(13) Å $\beta = 114.655(9)^{\circ}$ c = 17.750(5) Å $\gamma = 90^{\circ}$	a = 16.299(2) Å $\alpha = 90^{\circ}$ . b = 5.7664(6) Å $\beta = 92.692(5)^{\circ}$ c = 16.537(2) Å $\gamma = 90^{\circ}$
Volume	1553.0(7) Å <sup>3</sup>	1552.5(3) Å <sup>3</sup>
Z	4	4
Calculated density	1.255 Mg/m <sup>3</sup>	1.319 Mg/m <sup>3</sup>
Absorption coefficient	0.081 mm <sup>-1</sup>	0.091 mm <sup>-1</sup>
Crystal size	0.40 x 0.30 x 0.25 mm	0.55 x 0.50 x 0.30 mm
Reflections collected / unique	11739 / 3736 [R(int) = 0.0324]	11865 / 3752 [R(int) = 0.0359]
Data / restraints / parameters	3736 / 0 / 203	3752 / 0 / 211
Goodness-of-fit on F <sup>2</sup>	1.076	1.048
Final R indices [I > 2sigma(I)]	R1 = 0.0529, wR2 = 0.1432	R1 = 0.0491, wR2 = 0.1270
R indices (all data)	R1 = 0.0862, wR2 = 0.1731	R1 = 0.0849, wR2 = 0.1602

**Table S2.** Photophysical properties of **1**, **2**, and **3**

	<b>Compound 1</b>	<b>Compound 2</b>	<b>Compound 3</b>
$\lambda_{\max}$ abs(nm)	409 nm (pH 2.5)	434 nm(pH2.5)	318 nm
	355 nm (pH 6.5)	366 nm(pH6.5)	403 nm
	416 nm ( pH9.5)		
$\lambda_{\max}$ em(nm)	518 nm(pH 2.5), 560 nm (pH>8.5)	518 nm	604 nm
Stokes shift (nm)	151 nm	130 nm	176 nm
pKa	8.46	4.21, 9.51	–
$I_{\max}/I_{\min}$ (sensitivity)	15	55	–
Quantum yield	0.0014 (pH 8.20), 0.0025 (pH 9.04), 0.0057 (pH 10)	0.0005 (pH 4.03), 0.0018 (pH 6.50), 0.0013 (pH 8.20)	–
Molar absorption coefficient, ( $\text{ML}^{-1}\text{cm}^{-1}$ )	45400 ( $\lambda_{\max}$ =355, pH 4.75), 40100 ( $\lambda_{\max}$ =416, pH 10.75),	43600 ( $\lambda_{\max}$ =366, pH 4.75), 38680 ( $\lambda_{\max}$ =436, pH10.75)	–

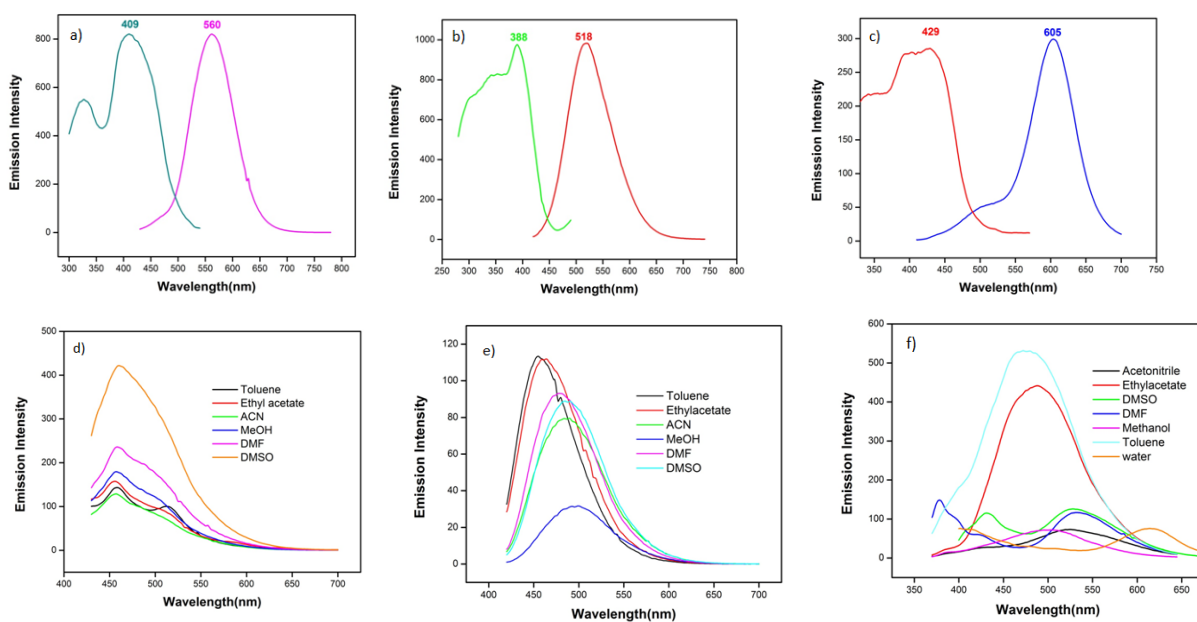


**Fig. S2.** Excitation and emission spectra of **1**, **2** & **3** in BR buffer ( $3.3 \times 10^{-5}$  M solution): a) **1**, b) **2**, c) **3**. Emission spectra of these compounds in various solvents ( $3.3 \times 10^{-5}$  M): d) **1** ( $\lambda_{\text{ex}}$  409 nm), e) **2** ( $\lambda_{\text{ex}}$  410 nm), and f) **3** ( $\lambda_{\text{ex}}$  380 nm).



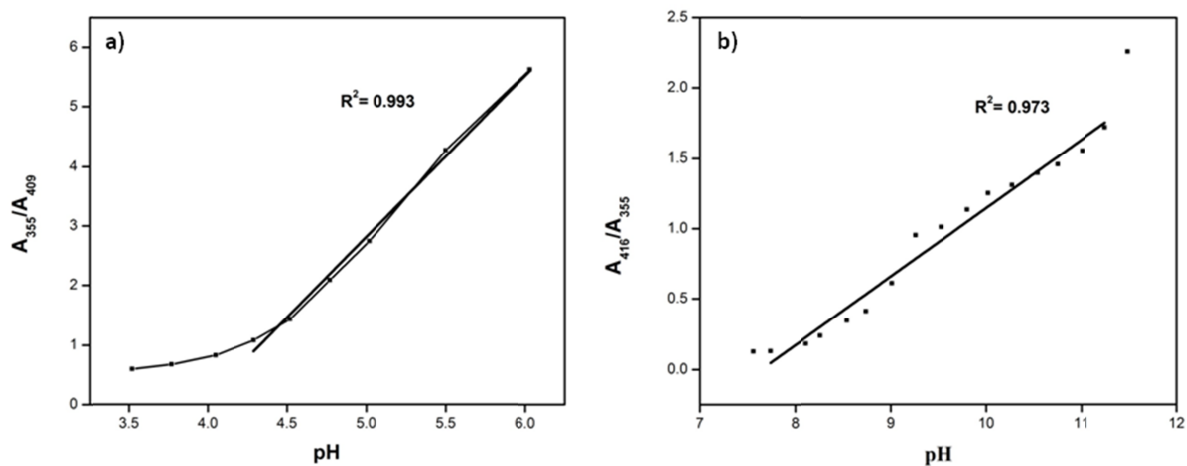


**Fig. S3.** Ratiometric response curves of **1** showing variation in (a)  $A_{355}/A_{409}$  and (b)  $A_{416}/A_{355}$  with pH.

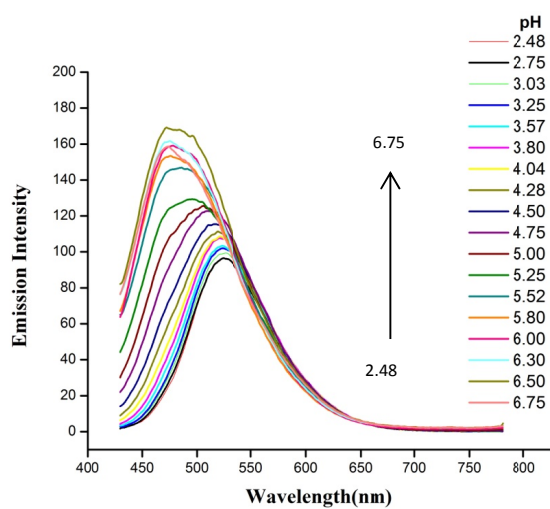


**Fig. S4.** Fluorescence emission spectra of **1** ( $\lambda_{\text{ex}}$ : 409nm,  $3.3 \times 10^{-5}$ M) in BR buffer at various pH (pH 2.5-6.75).

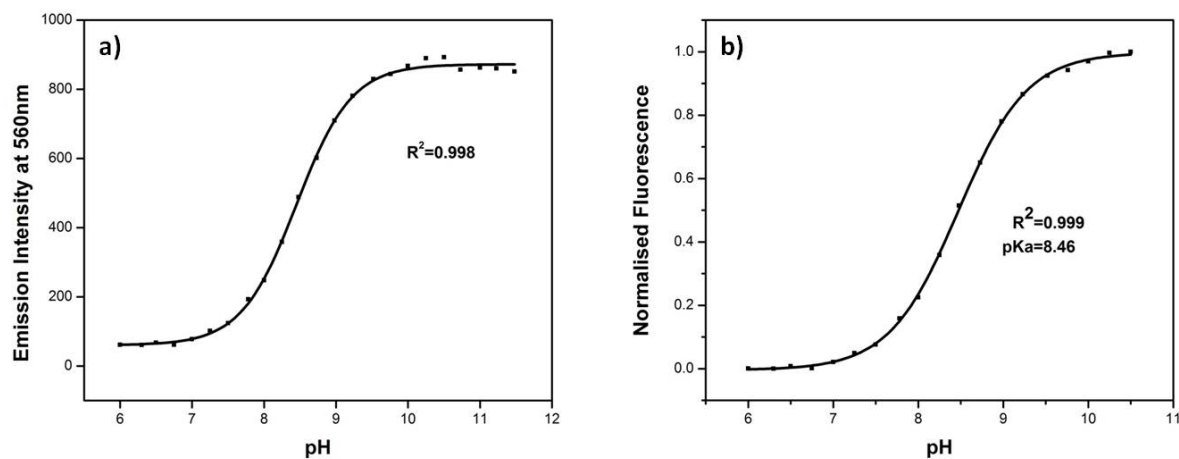


**Fig. S5.** (a) Change in emission intensity ( $\lambda_{\text{ex}}$  409 nm,  $\lambda_{\text{em}}$  560nm) of  $3.3 \times 10^{-5}$ M solution of **1** with pH; b) Plot of normalized fluorescence vs. pH. When the of normalized fluorescence  $I_n/I_{\text{max}} = 0.5$ , the corresponding pH is equal to pKa.

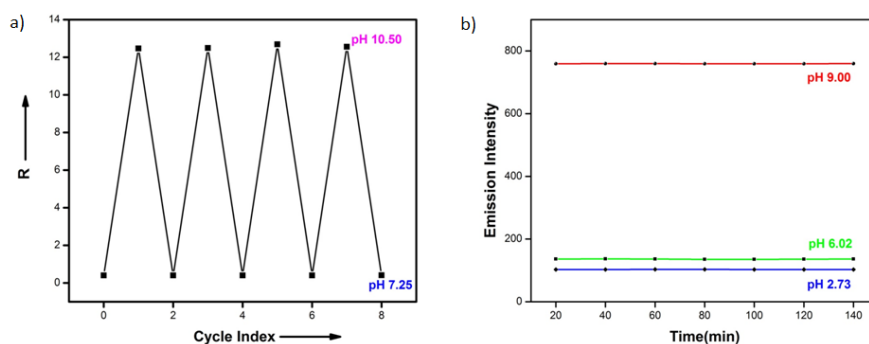


**Fig. S6:** (a) Cycle index of **1** between pH 7.25 and 10.5. The fluorescence emission intensity ratio ( $R = I_{560}/I_{475}$ ) was monitored by alternate addition of 2M HCl and 2M NaOH under excitation at 409 nm; b) Time dependent fluorescent emission intensities of  $3.3 \times 10^{-5}$ M of **1** in BR buffer at pH 2.73 ( $\lambda_{\text{em}}$  524 nm), 6.02 ( $\lambda_{\text{em}}$  475 nm) and 9.0 ( $\lambda_{\text{em}}$  560 nm) for 140 min ( $\lambda_{\text{ex}} = 409$  nm).

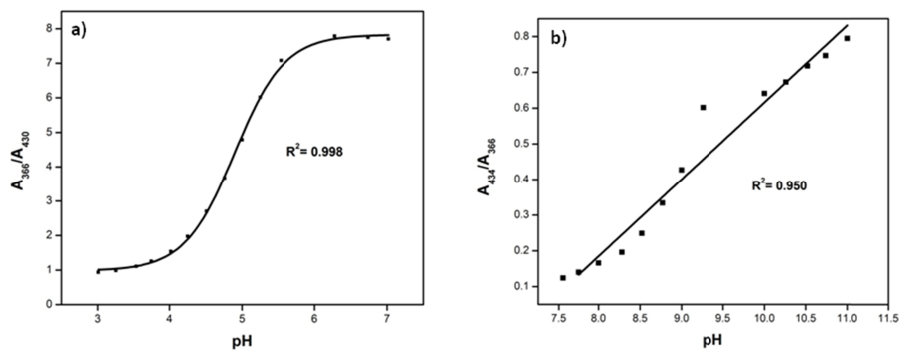


**Fig. S7.** Ratiometric response curve of **2** showing variation in a)  $A_{366}/A_{430}$  and b)  $A_{434}/A_{366}$  with pH.

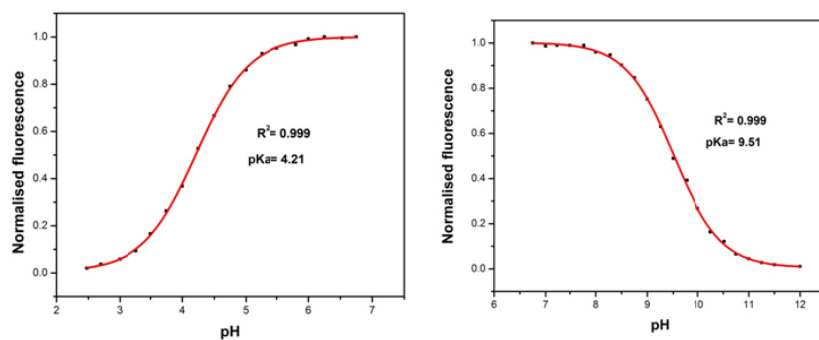


**Fig. S8.** Plot of normalized fluorescence intensity vs pH for compound **2**.

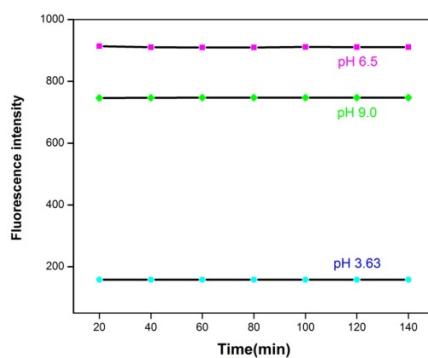


**Fig. S9.** Time dependent fluorescent emission of  $3.3 \times 10^{-5}$  M solution of **2** in BR buffer at pH 3.63, 6.5 and 9.0 for 140 min ( $\lambda_{\text{ex}} = 410$  nm and  $\lambda_{\text{em}} = 518$  nm).

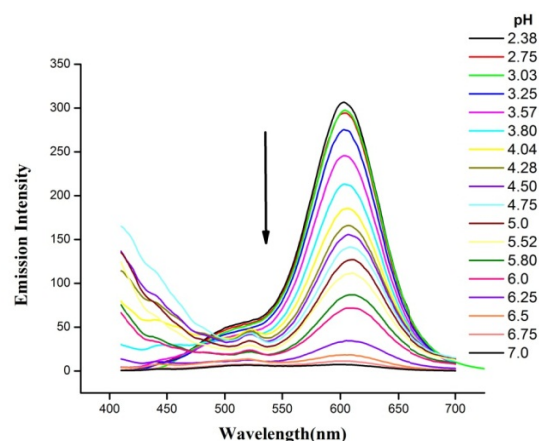


**Fig. S10.** Fluorescence emission spectra of  $3.3 \times 10^{-5}$ M solution of **3** ( $\lambda_{\text{ex}}$ : 380 nm, pH 2.55) in BR buffer

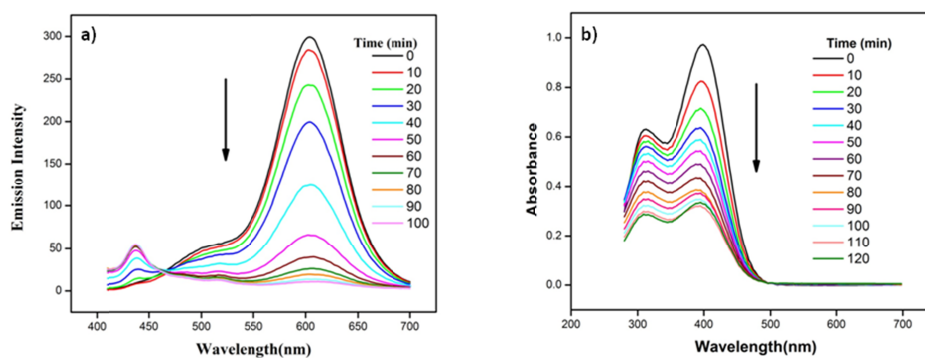


**Fig. S11.** a) Time-dependent emission and b) absorption spectra of **3** in BR buffer ( $3.3 \times 10^{-5}$ M, pH 2.50,  $\lambda_{\text{ex}}$  380 nm).

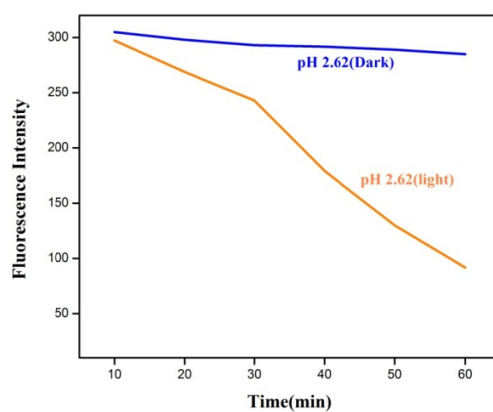


**Fig. S12.** Time-dependent changes in the intensity of fluorescent emission of **3** ( $3.3 \times 10^{-5}$ M) in BR buffer at pH 2.62 for 60 min ( $\lambda_{\text{ex}}$  = 480 nm and  $\lambda_{\text{em}}$  = 605 nm).

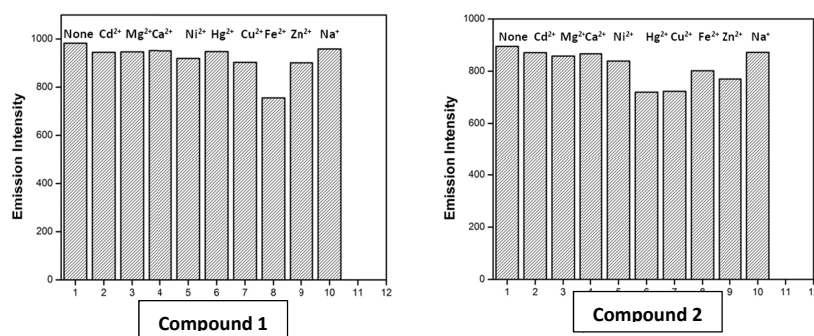


**Fig S13.** Fluorescence intensities of solutions of **1** & **2** in BR buffer ( $3.12 \times 10^{-3}$ M) in presence of various metal ions (10 equivalents): a) **1** ( $\lambda_{\max \text{ em}}$  560 nm, at pH 10.55) and b) **2** ( $\lambda_{\max \text{ em}}$  518 nm at pH 6.80).

## Cytotoxicity and Dose Response Analysis of **2**

### Sample preparation

2 mg of **2** was dissolved in 40  $\mu$ l DMSO and made upto 2 ml using MEM supplemented with 10% FBS and antibiotics (pH = 7.2 – 7.4). The solution was sterilized by filtering through 0.22 $\mu$  Millex GP Millipore syringe filter. Various concentrations of **2** was prepared in MEM ranging from 1-0.001 mg/ml.

### Cell culture

The cytotoxicity of **2** was evaluated by measuring the activity of the cells that are exposed to the compound **2**. L-929 cells were maintained in MEM supplemented with 10 % FBS and antibiotics with a medium change on every alternate days and monitored under an inverted phase contrast microscope (Nikon TES-100, Japan). Cells were subcultured using Trypsin-EDTA and seeded at a density of  $1 \times 10^4$  cells per well to a 96 well plate. When the cells reached subconfluency various dilutions of **2** was added to cells and incubated for 24 h inside a CO<sub>2</sub> incubator (Sanyo, Japan) set at  $37 \pm 1$  °C, 5% CO<sub>2</sub> and >90% relative humidity. Metabolic activity of the cells were determined by measuring the reduction of yellow colored MTT to purple colored formazan. Cells cultured in normal medium was considered as cell control and cells exposed to DMSO prepared similar to **2** was considered as reagent control. The test and control medium were replaced with 100 $\mu$ l MTT solution (1mg/ml in MEM without supplements) and incubated inside CO<sub>2</sub> incubator for 2 h. The MTT was removed and the formazan product formed was dissolved in 100  $\mu$ l isopropanol. The metabolic activity was determined by obtaining the absorbance of color

developed at 570 nm in a multiwell plate reader (Biotek, USA). Data was expressed as percentage of control cells

## In vitro evaluation of 2

### a. Experiment 1 - Cytotoxicity

To find the cytotoxicity of 2, L-929 cells were exposed to various concentrations of 2 ranging from 0.5 – 0.004 mg/ml. It was found that 0.5 mg/ml elicited a toxic response by presenting only 46.26 % of metabolic activity (Table S3). All the rest of the concentrations of 2 were found to be non-cytotoxic from 0.25 – 0.004 mg/ml (Figure S13).

**Table S3.** Cytotoxicity of 2 to L-929 cells at concentration range of 0.5 – 0.004 mg/ml.

Con (mg/ml)	0.500	0.250	0.125	0.063	0.031	0.016	0.008	0.004
% Activity (Avg)	46.26	105.79	124.10	127.11	123.08	120.07	118.77	118.97
SD	2.7	6.7	8.9	3.5	6.4	3.4	3.2	7.4

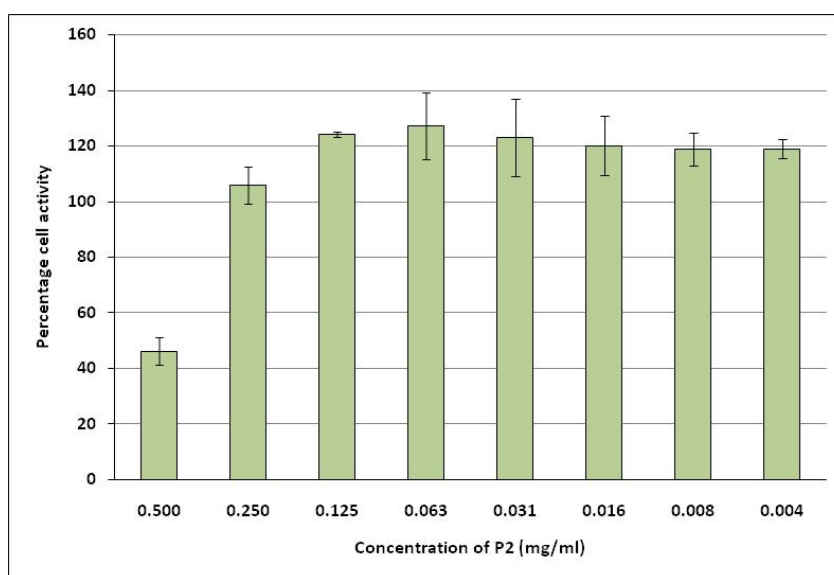


**Fig. S14.** Cytotoxicity of 2 to L-929 cells determined by MTT assay.

### b. Experiment 2 – Dose response

The dose response of L-929 cells to 2 was estimated by MTT assay by exposing cells to concentrations ranging from 1 mg/ml to 0.01 mg/ml (Figure S14). The cells expressed decreasing levels of cytotoxicity with respect to increasing levels of dilutions. The characteristic spindle morphology of L-

929 cells was evident in the lowest dose of **2** ie: 0.1 mg/ml. The cells exposed to **2** at highest dose of 1 mg/ml, showed cytotoxic pattern with round morphology, cell lysis and disruption of monolayer.

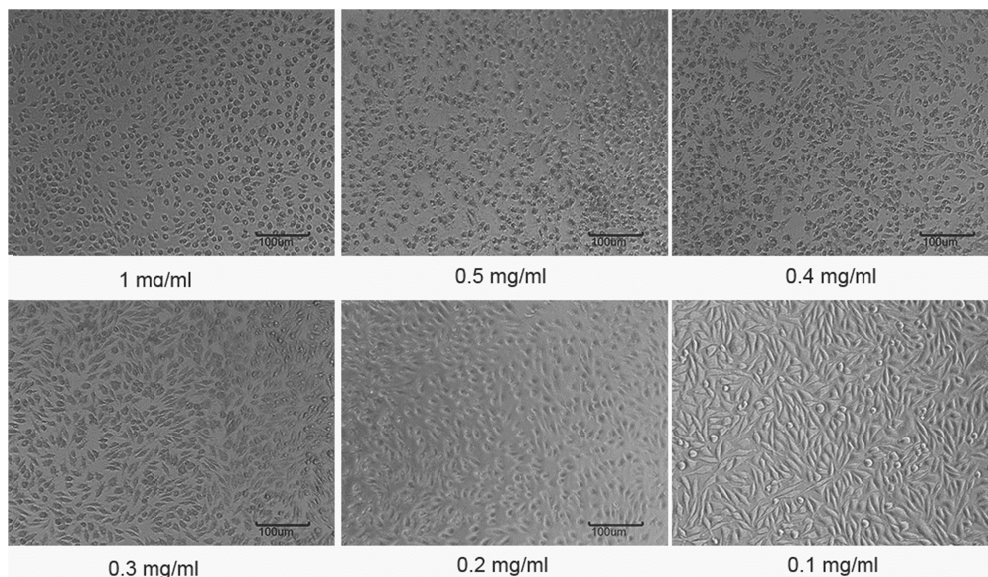


**Fig. S15.** Cells observed under microscope after exposing to various dilutions of **2**.

Metabolically active cells convert MTT to insoluble purple formazan crystals. When L-929 cells were exposed to **2** in culture medium at different dilutions, the formation of formazan was relative to the dose applied (Figure S15).

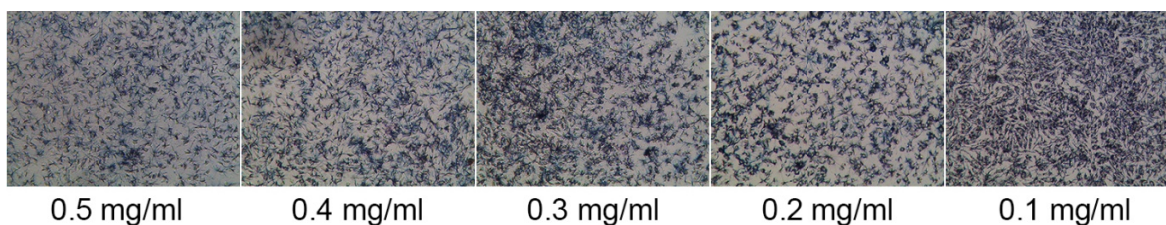


**Fig. S16.** Formazan product produced by the cells that are exposed to **2** for 24 h

At 1 mg/ml, the metabolic activity of **2** was 38 % which increased with dilution and reached 93.5 % at 0.01 mg/ml (Table S4 and Figure S16). The metabolic activity of reagent control (DMSO) was  $91.54 \pm 4.9$  % compared to cell control (Culture medium).

**Table S4:** Dose response of L-929 cells to **2** analyzed by MTT assay.

Con (mg/ml)	1.00	0.50	0.40	0.30	0.20	0.10
% Activity (Avg)	38.04	53.31	59.98	69.99	73.67	93.51
SD	6.7	0.8	11.8	13.9	10.8	5.7

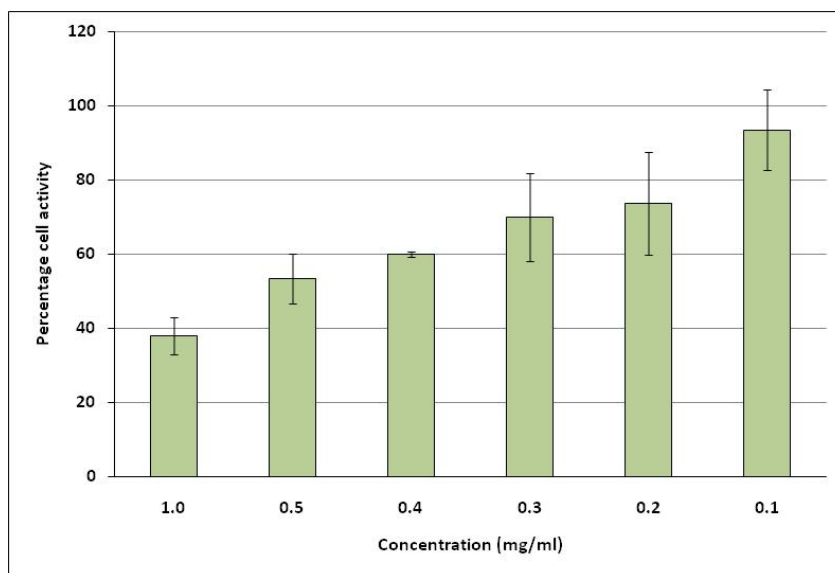


**Fig. S17.** MTT assay of L-929 cells exposed to **2** at concentration range of 1 – 0.1 mg/ml.

The concentration of **2** that gives a response of half activity between the highest and the lowest readings is designated as  $IC_{50}$  value. The  $IC_{50}$  estimated for **2** on L-929 cells was 0.328 mg/ml (Figure S17).

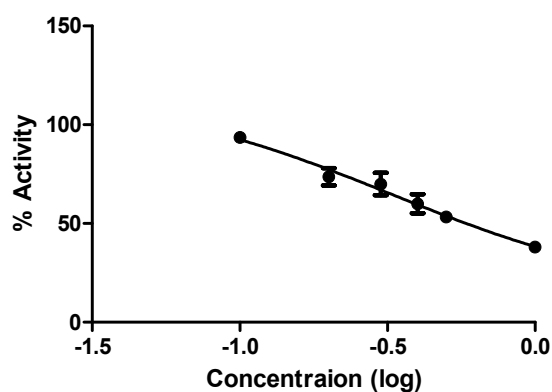


**Fig. S18:** Dose response of L-929 cells to **2**. x axis is the log of concentrations used and y axis represents the percentage cell activity



## Uptake of compound **2** in HepG2 cells

### Cell culture and uptake study

HepG2 cells were cultured in MEM supplemented with 10% FBS, antibiotic and incubated at 37°C under a humidified atmosphere containing 5% CO<sub>2</sub>. The pH of the medium was 7.2-7.4 throughout the experiment as visualized by the red colour of phenol red indicator. Cells were harvested using trypsin and seeded on glass coverslips at a density of  $1 \times 10^5$  cells/cm<sup>2</sup> and allowed to reach subconfluency.

In order to study the cellular uptake, stock solution of **2** was prepared by dissolving 5 mg **2** in 100  $\mu$ l DMSO. The stock solution was diluted with MEM (pH = 7.2 – 7.4) supplemented with 10% FBS and antibiotics to get a concentration of 0.1 mg/ml. The solution was sterilized by filtering through 0.22  $\mu$ m poresize syringe filter (Millex GP, Millipore). HepG2 cells were exposed to **2** and cellular uptake was determined after 2 h and 12 h. Cells were fixed in buffered formalin solution for 30 min and cell nucleus was counter stained with PI (1  $\mu$ g/ml in PBS) for 1 min. Cells cultured in normal medium without **2** was considered as negative control. Cellular uptake was analyzed under a Laser Scanning Confocal Microscope (LSM 510 Meta, Carl Zeiss, Germany) with simultaneous acquisition of **2** and PI fluorescence. **2** uptake was imaged by illuminating with 405 Blue diode laser and different band pass emission filters such as 420-480 nm, 470-500 nm and 505-530 nm. Cell nucleus was detected by exciting samples with HeNe - 543 laser and long pass 560 nm emission filter.

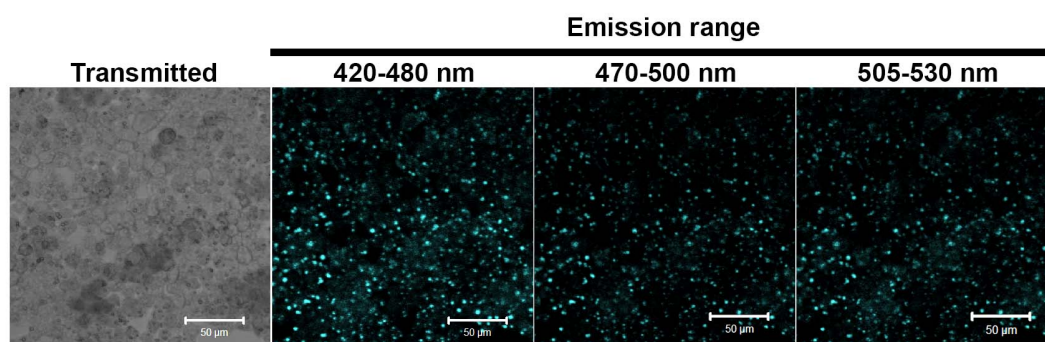


**Fig. S19.** Confocal images showing uptake of **2** by HepG2 cells observed after 2h exposure. The samples were excited with 405 nm and the emissions were captured at different bandpass filters.

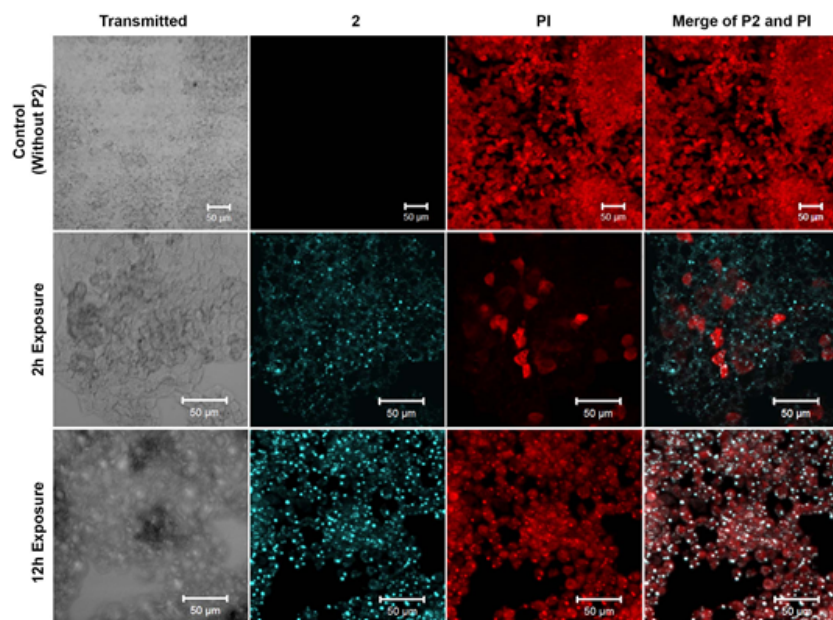


**Fig. S20.** Cellular uptake analysis of **2** with HepG2 cells observed under confocal microscope after 2 and 12 h exposure. Blue colour represents **2** uptake and red portions denotes PI from counter staining. The presence of **2** was detected as early as 2h and the internalization continued as evidenced by increased fluorescence signal at 12 h.

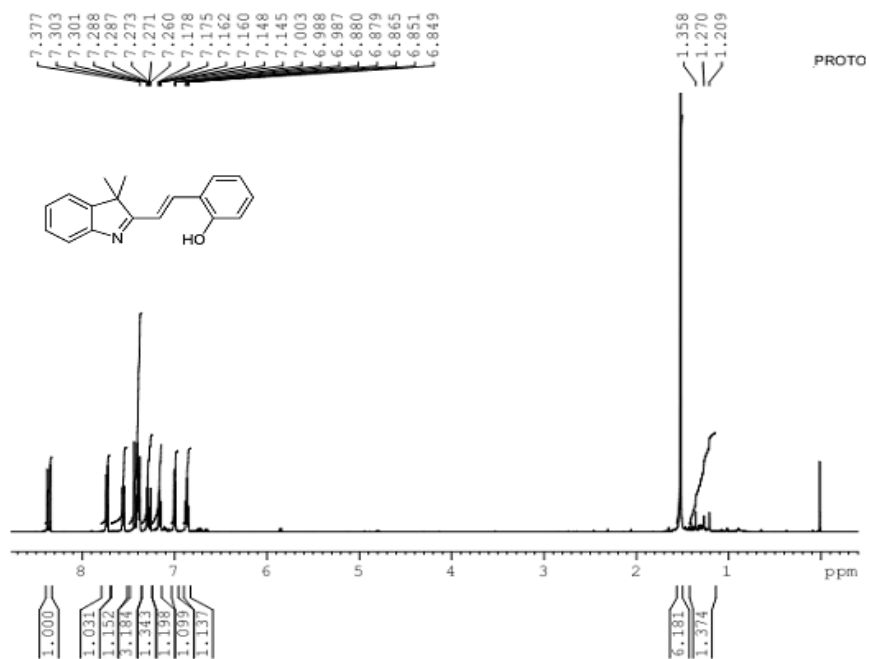


Fig. S21. <sup>1</sup>H NMR of **1** (500 MHz, CDCl<sub>3</sub>).

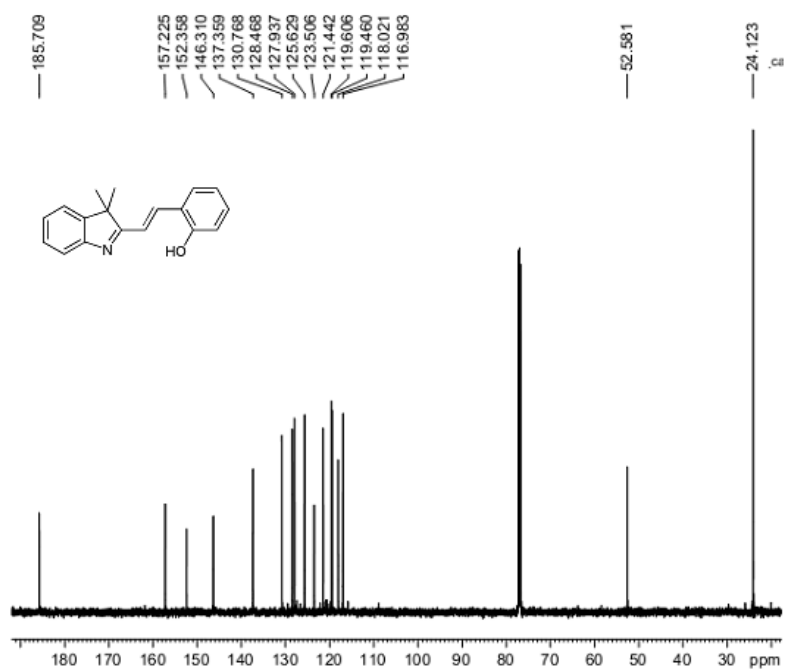


Fig. S22. <sup>13</sup>C NMR of **1** (125 MHz, CDCl<sub>3</sub>).

S19

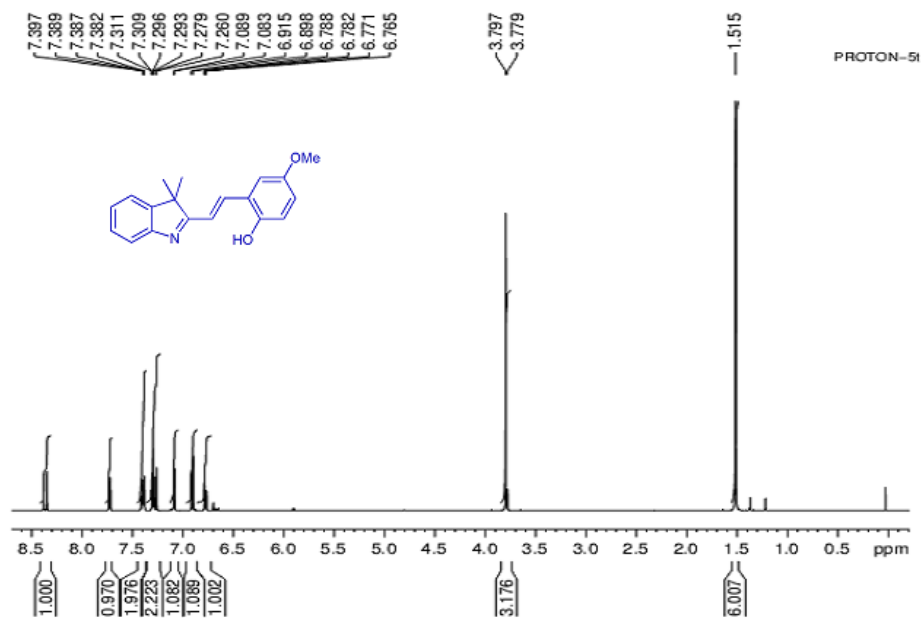


Fig. S23.  $^1\text{H}$  NMR of **2** (500 MHz,  $\text{CDCl}_3$ ).

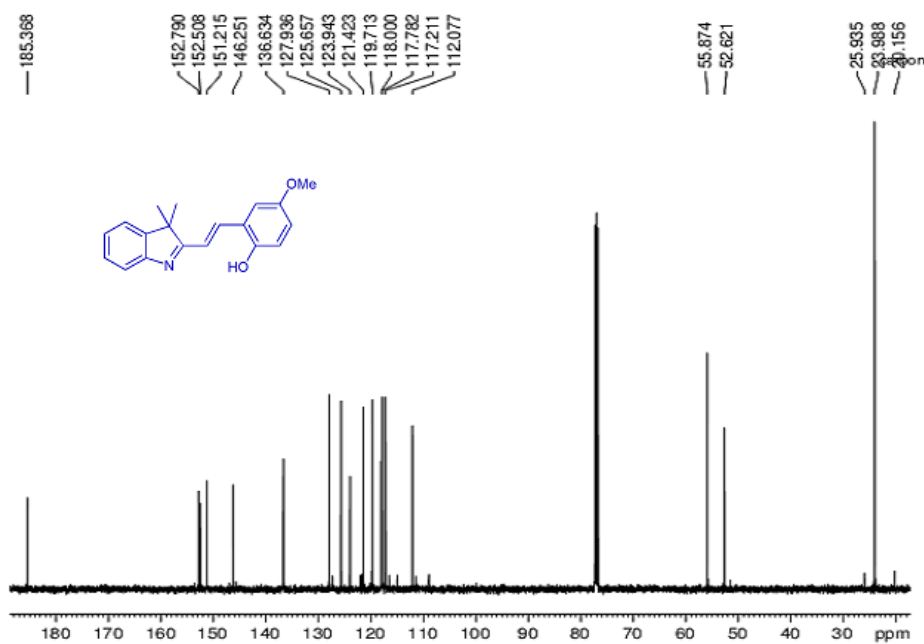


Fig. S24. <sup>13</sup>C NMR of 2 (125MHz, CDCl<sub>3</sub>).

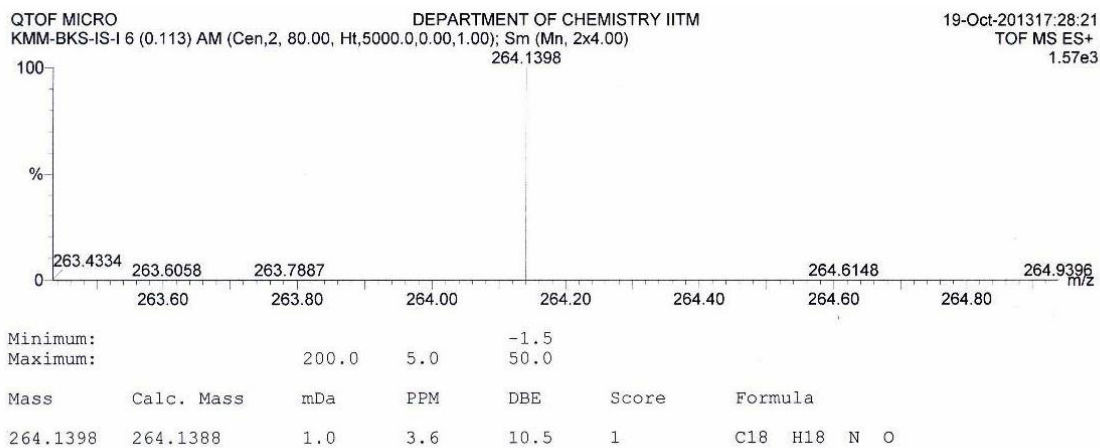
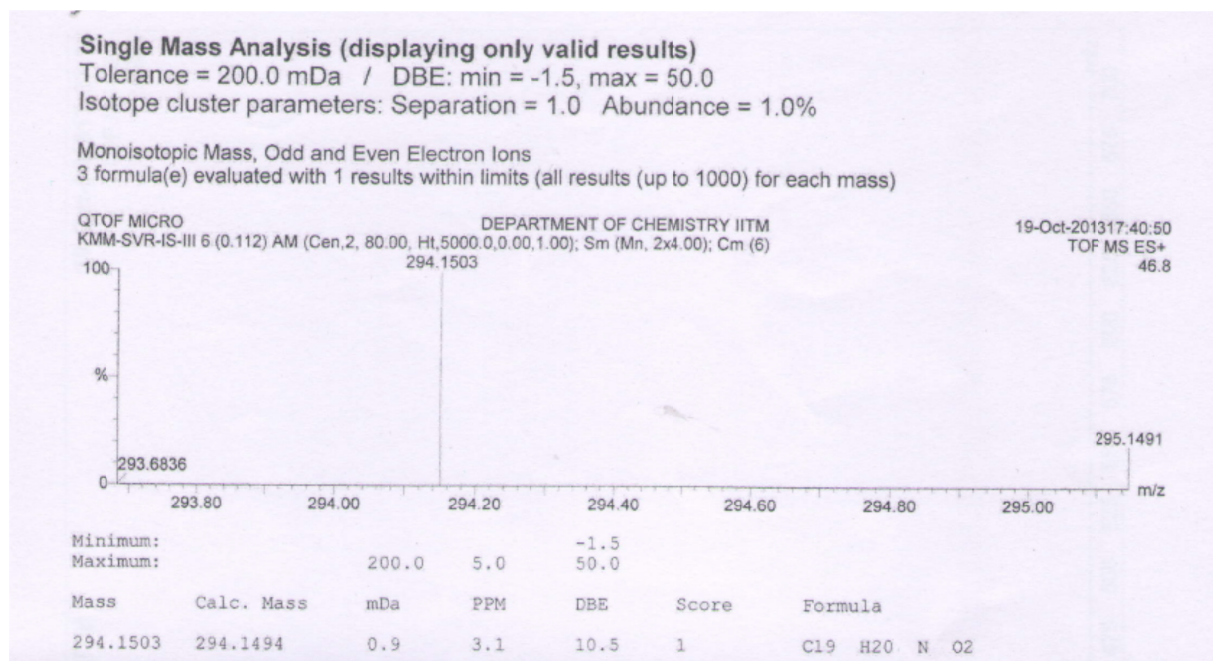


Fig. S25. HRMS of 1.



**Fig. S26.** HRMS of 2.